

**Exploring NLS1 through the physical properties of their hosts<sup>1</sup>**V. Botte<sup>2</sup>, S. Ciroi<sup>2</sup>, P. Rafanelli and F. Di Mille*Department of Astronomy, University of Padova, vicolo dell'Osservatorio 2, I-35122 Padova, Italy***ABSTRACT**

In this work we aim at addressing the still open question about the nature of Narrow-Line Seyfert 1 (NLS1) galaxies: are they really active nuclei with lower mass Black-Holes (BHs) than Seyfert 1 (S1) and quasars? Our approach is based on the recently discovered physical connections between nuclear supermassive BHs and their hosting spheroids (spiral bulges or ellipticals). In particular we compare BH masses of NLS1s and S1s analyzing the properties of their hosts by means of spectroscopic and photometric data in the optical wavelength domain. We find that NLS1s fill the low BH mass and bulge luminosity values of the  $\mathcal{M}_{\text{BH}} - M_{\text{B}}$  relation, a result strongly suggesting that NLS1s are active nuclei where less massive BHs are hosted by less massive bulges. The correlation is good with a relatively small scatter fitting simultaneously NLS1s, S1s and quasars. On the other hand, NLS1s seem to share the same stellar velocity dispersion range of S1s in the  $\mathcal{M}_{\text{BH}} - \sigma_*$  relation, indicating that NLS1s have a smaller BH/bulge mass ratio than S1s. These two conflicting results support in any case the idea that NLS1s could be young S1s. Finally we do not confirm the significantly non linear BH–bulge relation claimed by some authors.

*Subject headings:* galaxies: active — galaxies: nuclei – galaxies: bulges – galaxies: Seyfert – (galaxies:) quasars: general

**1. INTRODUCTION**

Narrow-Line Seyfert 1 (NLS1) galaxies belong to the family of active galactic nuclei (AGNs) and owe their name to the peculiar properties that distinguish them from the other type 1 AGNs. In general a Seyfert 1 (S1) is classified as NLS1 when its nuclear spectrum shows the permitted lines only slightly broader ( $\text{FWHM}(\text{H}\beta) < 2000 \text{ km s}^{-1}$ ) than the forbidden ones (Osterbrock &

---

<sup>2</sup>Guest investigator of the UK Astronomy Data Centre

<sup>1</sup>Partially based on observations made with the Asiago 1.82 m telescope of the Padova Astronomical Observatory

Pogge 1985). But NLS1 galaxies are characterized also by a strong Fe II emission, a soft X-ray slope steeper than the slope typical for S1 galaxies, rapid and large soft X-ray variability (Boller, Brandt & Fink 1996), a weak Big Blue Bump in the optical/UV range, likely shifted toward higher energies (Pounds et al. 1987), a bright IR emission and a nuclear super-solar metallicity (Mathur 2000; Komossa & Mathur 2001).

Even though NLS1s are known since almost twenty years (Osterbrock & Pogge 1985), their nature is still a matter of debate. For example, at present the reason of the narrowness of broad permitted lines in NLS1s is not clear. Boller et al. (1996) suggested that if the gravitational force from the central Black-Hole (BH) is the main cause of motion of the Broad Line Region (BLR) clouds, narrower optical emission lines will result from smaller  $\mathcal{M}_{\text{BH}}$  ( $\sim 10^6 - 10^7 \mathcal{M}_{\odot}$ ) provided the BLR distance from the central source does not change strongly with  $\mathcal{M}_{\text{BH}}$ . These BHs with smaller masses are expected to accrete matter at near or super-Eddington rates in order to maintain the relatively normal observed luminosities. Recently Mathur et al. (2001) proposed that NLS1s may be relatively young AGNs hosting BHs still in a growing phase. Nevertheless other authors suggested that if the BLR clouds were largely confined to a plane, as it seems to happen in radio-loud AGNs (see e.g. McLure & Dunlop 2002, and references therein), NLS1 galaxies could be simply a case in which their BLR is observed more face-on than in S1s (see e.g. Osterbrock & Pogge 1985). Smith et al. (2002) pointed out that also a partly obscured BLR could justify narrow permitted lines, but these last two scenarios should produce polarization. They claimed that H $\alpha$  polarization properties of the NLS1s are indistinguishable from those of S1s, excluding obscuration of the inner regions of BLR or a face-on orientation of a disk-like BLR as the explanation for the relatively narrow broad-line profiles.

The connection between physical properties of nuclear supermassive BHs and their host galaxies, on which several works have focused in the last years, might turn out to be a powerful tool to understand the nature of NLS1s and settle the above cited controversies. Kormendy & Richstone (1995) first found out a correlation between BH mass ( $\mathcal{M}_{\text{BH}}$ ) and the absolute B magnitude of the spheroidal component ( $M_B$ ). Magorrian et al. (1998) determined  $\mathcal{M}_{\text{BH}}$  values for a sample of 32 nearby galaxies and suggested that  $\mathcal{M}_{\text{BH}}$  is proportional to the  $\mathcal{M}_{\text{bulge}}$  such that on average  $\mathcal{M}_{\text{BH}}/\mathcal{M}_{\text{bulge}} \sim 0.005$ . Other authors estimated a similar mass ratio,  $\sim 0.002$  (see e.g., Ho 1999). Recently, studying a sample of nearby galaxies Gebhardt et al. (2000a), Ferrarese & Merritt (2000) and Tremaine et al. (2002) have shown that  $\mathcal{M}_{\text{BH}}$  is tightly correlated with the velocity dispersion of the bulge stellar component ( $\sigma_*$ ), although they disagreed about the value of the slope.

In AGNs as well, BHs are also expected to correlate with their host bulges. This possibility was explored on a sample of PG quasars by Laor (1998) who found agreement with the relation of Magorrian et al. (1998). Later Wandel (1999) claimed that Seyfert galaxies show on average a  $\mathcal{M}_{\text{BH}}/\mathcal{M}_{\text{bulge}}$  ratio systematically lower than that for normal galaxies and quasars. Conversely Gebhardt et al. (2000b) included in their work seven AGNs for which the  $\mathcal{M}_{\text{BH}}$  were obtained by means of the reverberation mapping technique. They found that these objects were in agreement with their previously found  $\mathcal{M}_{\text{BH}}-\sigma_*$  correlation. Further support came from McLure & Dunlop

(2001), and from Wu & Han (2001) who studied samples of quasars and Seyfert galaxies, and did not find any evidence that Seyfert galaxies follow a different  $\mathcal{M}_{\text{BH}} - \mathcal{M}_{\text{bulge}}$  relation from quasars or nearby galaxies.

Until now no agreement has been found about NLS1s. Mathur, Kuraszekiewicz & Czerny (2001) and very recently Bian & Zhao (2003a) and Grupe & Mathur (2004) showed that the  $\mathcal{M}_{\text{BH}}/\mathcal{M}_{\text{bulge}}$  ratio in NLS1s is significantly smaller than that for Seyfert galaxies. Conversely Wang & Lu (2001), studying a sample of 59 NLS1s observed spectroscopically by Véron-Cetty, Véron & Gonçalves (2001), found that there is non clear difference in the  $\mathcal{M}_{\text{BH}}-\sigma_*$  relation (where  $\sigma_*$  is represented by the [O III] emission line width) between NLS1s, Broad-Line AGNs and nearby galaxies.

Our purpose in this work is to investigate the nature of NLS1s by exploring the physical properties of their bulges, namely the luminosity and the nuclear stellar velocity dispersion. Our approach makes use of both new observational data and data from the literature. The necessary corrections are applied to the latter in order to obtain as homogeneous as possible a dataset. Furthermore, as a main difference with respect to several other works on this topic, when determining the bulge properties of the host galaxies we take into account the influence of the AGN, which, as we show, can be non-negligible and affect the results considerably. The structure of the paper is as follows: in §2 we present our dataset and derive and compare BH mass values for a sample of NLS1s and S1s. In §3 we estimate the blue absolute magnitudes and the stellar velocity dispersions of their bulges. Our results are summarized and discussed in §4.

## 2. BLACK-HOLE PROPERTIES

### 2.1. Spectroscopic data

Firstly, we have isolated a list of 23 NLS1 and 23 S1 galaxies of the northern emisphere from Véron-Cetty et al. (2001) on the basis of their “S1n” and “S1.0” classification and of the redshift,  $z < 0.1$ , chosen to avoid that  $\text{H}\beta$  and [O III] lines fall in a spectral region with strong night-sky emission lines.

No other selection criteria were applied. This sample is complete up to visual magnitude 15.5, corresponding to the 80 per cent of the selected galaxies, and therefore it is useful for our purposes. Out of this sample, we were able to collect optical spectra for 22 NLS1s and 15 S1s. In particular 19 NLS1s and 7 S1s were extracted from the public data available in the Isaac Newton Group (ING) Archive. These spectra were obtained for different purposes in 1995, 1996, 1999 and 2000, mostly with the Intermediate Dispersion Spectrograph (IDS) mounted at the 2.5m Isaac Newton Telescope (INT, Canary Islands, Spain), and the others with the ISIS Double Beam Spectrograph (ISIS) at the 4.2m William Herschel Telescope (WHT, Canary Islands, Spain). Other 3 NLS1s and 8 S1s were observed directly by us in 2002 September and in 2003 January using the Asiago Faint Object Spectrograph and Camera (AFOSC) mounted at the 1.82m telescope of the Padova Astronomical Observatory (Asiago, Italy). Tables 1 and 2 summarize the instrumental setup and

the total wavelength coverage for each observation.

All spectra were reduced with the same procedure. The usual data reduction steps - bias and flat field corrections, cosmic rays removal, wavelength linearization, sky-background subtraction and flux calibration- were carried out with IRAF packages<sup>2</sup>. A one-dimensional spectrum of the nucleus was obtained for each galaxy summing a number of pixels along the spatial direction on the basis of the seeing conditions. When available, adjacent spectral ranges of the same source were combined together. Then a correction for Galactic extinction was applied using for each galaxy the value given by NED<sup>3</sup> and the Cardelli, Clayton, & Mathis (1989) extinction law. The so-processed spectra were shifted to the rest frame and the intrinsic absorption was removed following the technique used by Crenshaw et al. (2002). In particular we have determined the value of the internal reddening using the relation:  $E(B - V) = 2.5 [\log(X_B) - \log(X_V)]$ , where  $X$  is the ratio of the Mrk 478 continuum fit to that of the other galaxies of the sample evaluated at the effective wavelengths of B (4400 Å) and V (5500 Å) photometric bands. Contrary to Crenshaw et al. (2002) we could not use as reference Mrk 493, whose spectrum was available only for wavelengths  $> 4400\text{Å}$  thus yielding a rather uncertain estimate of  $X_B$ . The spectrum of Mrk 478 was used, instead, after correction for internal absorption by means of the hydrogen column density  $N_H = 2.0 \pm 10^{20} \text{ cm}^{-2}$ , given by Boller et al. (1996).

One of the peculiar features in the optical spectrum of most NLS1 galaxies is the presence of strong emission of Fe II multiplets centered at 4570 Å, 5190 Å and 5300 Å. In order to remove them and allow a more precise measure of  $H\beta$  and [O III] emission lines we have produced a Fe II template using the spectrum of the NLS1 I Zw 1 as suggested by Boroson & Green (1992). The template was scaled in intensity and conveniently smoothed to match the spectrum of each galaxy showing evident Fe II multiplets, and then subtracted.

## 2.2. Wrong classifications

A fast inspection of each galaxy spectrum allowed us to isolate four NLS1s, Mrk 1126, Mrk 291, Mrk 957 and HB 1557, which in our opinion are wrongly classified. After a multi-gaussian fit of  $H\beta$ , and  $H\alpha + [\text{N II}] \lambda\lambda 6548, 6583$  emission lines we can assert that these active nuclei have permitted lines with a clear composite broad+narrow profile, where the narrow components have widths similar to those of the forbidden lines ( $\sim 250 - 300 \text{ km s}^{-1}$ ) (Fig. 1). This kind of profile is typically shown by intermediate Seyfert galaxies. Indeed Osterbrock (1989) introduced the notation Seyfert 1.5, 1.8, and 1.9, to indicate the simultaneous presence of narrow and broad permitted lines in many spectra of Seyfert galaxies.

---

<sup>2</sup>IRAF is written and supported by NOAO (Tucson, Arizona), which is operated by AURA, Inc. under cooperative agreement with the National Science Foundation

<sup>3</sup>NASA Extragalactic Database

Broad  $H\beta$  and  $H\alpha$  components were fitted in Mrk 1126 and Mrk 291, obtaining widths of about 2600-2900  $\text{km s}^{-1}$ , while only  $H\alpha$ -broad was detected in Mrk 957 and HB 1557, and fitted to widths of about 1600 and 3000  $\text{km s}^{-1}$  respectively. We observe that the value of  $H\alpha$ -broad in Mrk 957 is lower than the others. This could be caused by a non reliable multigaussian fit of  $H\alpha + [\text{N II}]$  blend. Indeed we have the impression that a blue  $[\text{N II}]$  component exists in addition to the others already identified, but the spectral resolution is not sufficiently high to obtain a stable fit of the profile with six or more gaussians. Moreover we noted that Mrk 957 is the only out of the four galaxies showing Fe II multiplets, whose strong emission is one of the typical features of NLS1s.

Therefore we excluded these four galaxies from our sample of NLS1s, but we included UGC 3478 until now wrongly classified as S1. UGC 3478 has an optical nuclear spectrum typical of NLS1s: we have found narrow Balmer emission lines ( $\text{FWHM}(H\beta) = 1600 \text{ km s}^{-1}$ ), a low  $[\text{O III}] \lambda 5007 / H\beta$  ratio ( $= 4.8$ ), and a strong emission of  $[\text{Fe II}]$  multiplets. Moreover the luminosities of the low ionization emission lines,  $[\text{N II}] \lambda 6583$ ,  $[\text{S II}] \lambda \lambda 6716, 6731$  and  $[\text{O I}] \lambda 6300$ , assume weak values. The ASCA hard X-ray spectrum, available in TARTARUS database, shows a steep power law distribution with photon index  $\Gamma_X \sim 2.3$  similar to that given by Leighly (1999) for NLS1s ( $\Gamma_X \sim 2.19 \pm 0.10$ ).

### 2.3. BH masses estimation

The stellar dynamical techniques to derive BH masses are severely limited for AGNs, since they require high S/N measurements of stellar absorption features which are often lost in the glare of a bright active nucleus (Nelson 2000). The alternative solution consists in applying the virial theorem to the BLR clouds, gravitationally bound to the central mass and located at distances of few light-days (S1s) to several light-weeks (quasars):

$$\mathcal{M}_{\text{BH}} = R_{\text{BLR}} V^2 G^{-1} \quad (1)$$

where  $R_{\text{BLR}}$  is the radius of the BLR,  $V$  the velocity of the broad-line emitting gas, and  $G$  the gravitational constant. Even if there is no general consensus about the dynamics of the BLR, evidence for Keplerian motions of the BLR clouds was found by Peterson & Wandel (1999) and Wandel, Peterson & Malkan (1999) using the reverberation mapping technique. This is one of the major tools for studying correlated variations of the lines and continuum emission of AGNs and determine the size ( $R_{\text{BLR}}$ ) and the geometry of the BLR (see e.g., Peterson 1993).

However, the lack of long term variability monitoring makes it difficult to measure  $R_{\text{BLR}}$  of most Seyfert galaxies using this method. As an alternative,  $R_{\text{BLR}}$  can be estimated by the empirical relationship between the BLR size and the luminosity of the continuum at  $5100\text{\AA}$  found by Kaspi et al. (2000):

$$R_{\text{BLR}} = 32.9_{-1.9}^{+2.0} \left[ \frac{\lambda L_{\lambda}(5100\text{\AA})}{10^{44} \text{ erg s}^{-1}} \right]^{0.700 \pm 0.033} \quad (2)$$

Since the BLR consists of photoionized clouds of gas and the luminosities of NLS1s and S1s are generally comparable, (see e.g. Padovani & Rafanelli 1988; Boller et al. 1996), we applied this relation, whose validity for a few NLS1s was proved by Peterson et al. (2000). Indeed after having measured  $\lambda L_{\lambda}(5100\text{\AA})^4$  for each object of our sample we have verified that NLS1s and S1s have similar optical luminosity of continuum ( $\log \lambda L_{\lambda}(5100\text{\AA}) = 43.51 \pm 0.65$  vs.  $43.08 \pm 0.45$  respectively), as can be seen in Fig. 2.

Some authors produced substantial evidence that the broad-line emitting material has a flattened disk-like geometry in radio-loud quasars (see e.g., Vestergaard, Wilkes & Barthel 2000). Such evidence is less strong for radio-quiet AGNs, even if very recently Strateva et al. (2003) found that a high percentage of AGNs showing double-peaked Balmer lines are radio-quiet. Therefore, we have estimated the parameter  $V$  from the emission-line width of  $H\beta$  by assuming that the velocity dispersion in the line emitting gas is isotropic and after having removed the instrumental width:

$$V = (\sqrt{3}/2)\text{FWHM}(H\beta) \quad (3)$$

The resulting  $\mathcal{M}_{\text{BH}}$  values are listed in Tables 6 and 7. As expected NLS1s have on average BHs with smaller masses than S1s:  $\log \mathcal{M}_{\text{BH}} = 6.65 \pm 0.64$  vs.  $7.37 \pm 0.62$ , a result which depends directly on the narrowness of the Balmer emission lines, since nuclear luminosities and therefore BLR radii are quite similar in both samples. Similar considerations can be found in a contemporary paper by Grupe & Mathur (2004).

Of course such  $\mathcal{M}_{\text{BH}}$  values are characterized by some uncertainties, and we have tried to analyze them. First of all the uncertainties given in equation (2) produce errors  $< 15$  per cent concerning  $R_{\text{BLR}}$  calculated values. Second, the luminosity of the continuum is affected by flux calibration errors and by intrinsic variability of the sources. About this last point, following the discussion by Wang & Lu (2001), who noticed that the continuum variation is not larger than a factor of two for most AGNs, we assumed a 30 per cent error as upper limit. The spectrophotometry accuracy, evaluated through multiple observations of standard stars, was estimated around 10 – 20 per cent for archival data, and 20 – 30 per cent for Asiago data. Combining these errors together we obtain a  $< 40$  per cent error for  $R_{\text{BLR}}$ . The final uncertainty of  $\mathcal{M}_{\text{BH}}$  is likely less or around 50 per cent, corresponding to  $\sim 0.25$  dex in logarithmic scale. It should be taken into account that a non negligible fraction of optical light may come from the host galaxy, especially in case of low luminosity AGNs. Since a precise estimate of the host contribution is not straightforward, we decided to neglect it and remain closer to the procedure followed by Kaspi et al. (2000) to obtain their empirical relation.

---

<sup>4</sup>Throughout this paper we assume  $H_0 = 75 \text{ km s}^{-1} \text{ Mpc}^{-1}$ .

### 3. BULGE PROPERTIES

After having calculated the masses of the BHs hosted by each galaxy of our samples of NLS1s and S1s, we have investigated the physical properties of their bulges deriving their blue luminosities and the values of the central stellar velocity dispersion. Then we have explored the connection between bulges and nuclear BHs in order to find out where NLS1s are placed with respect to S1s.

#### 3.1. Blue luminosity

Since we did not have at our disposal photometric data to measure B-band magnitudes ( $m_B$ ), we took from literature, when available, the values for the objects of our samples (Winkler 1997; MacKenty 1990; Granato et al. 1993; Schmitt & Kinney 2000; Prugniel & Heraudeau 1998). When we found multiple estimates we calculated a median value.

The  $m_B$  were corrected for Galactic extinction ( $\Delta m_G$ ), taking values given by Schlegel, Finkbeiner & Davis (1998), and internal absorption ( $\Delta m_i$ ), following the relation given in the introduction to the Third Reference Catalogue of Bright Galaxies (de Vaucouleurs et al. 1991, RC3) :  $\Delta m_i = \alpha_T \log(\sec i)$ , where  $\alpha_T = 1.5 - 0.03 (T - 5)^2$  for spiral galaxies ( $T \geq 0$ ). Inclination values  $i$  were extracted from HyperLeda<sup>5</sup> database. The K correction was also applied ( $\Delta m_k$ ), again by following the method described in RC3.

Contrary to what done by several other authors, we decided to take into account the emission-line and non-stellar continuum contributions from the AGN to the total magnitude of each galaxy. To do this we followed the approximations given by Whittle (1992). In particular we used the formulae (2), (3), (4) and (5) given in that paper for  $F_{cF}$  and  $F_{cH}$ , which are the effective continuum fluxes in B-band due to the forbidden and Balmer emission lines. Instead, before calculating the nonstellar continuum flux  $F_{cC}$ , we noticed that Whittle (1992) assumed a typical value of  $\sim 100\text{\AA}$  as equivalent width of  $H\beta$ . Since we have the spectra and the underline continuum of  $H\beta$  is very similar to the already measured continuum at  $5100\text{\AA}$ , we could take as approximation  $F_{cC} \simeq F_\lambda(5100\text{\AA})$ , having adopted a power law with spectral index  $\alpha = -1.0$  as done by Whittle (1992). The total non stellar flux  $F_c = F_{cF} + F_{cH} + F_{cC}$  gives the required correction  $\Delta m_A$  to be applied to  $m_B$ . The final corrected total magnitudes are given by:  $m'_B = m_B + \Delta m_A - \Delta m_i - \Delta m_G - \Delta m_k$ .

The distribution of these terms are shown in Fig. 3. It can be easily noticed that  $\Delta m_k$  plays a minor role in the total contribution to the magnitude corrections, while  $\Delta m_A$  is as important as —and sometimes even more important—  $\Delta m_i$  and  $\Delta m_G$ . This strongly indicates that neglecting  $\Delta m_A$  can be a dangerous approximation when bright AGNs are considered.

After having converted  $m'_B$  into absolute magnitudes  $M_B$ , listed in Table 3, we obtained the

---

<sup>5</sup><http://leda.univ-lyon1.fr/>

bulge magnitudes ( $M_{B,bulge} = M_B + \Delta m_{bulge}$ ) by applying the formula given by Simien & de Vaucouleurs (1986), who found a relation between the bulge-to-total (B/T) luminosity ratio and the morphological type:  $\Delta m_{bulge} = 0.324 (T + 5) - 0.054 (T + 5)^2 + 0.0047 (T + 5)^3$ .

The morphology of each galaxy was extracted from NED and checked by visual inspection of the POSS II digitized images, for lower redshift sources, which did not require high spatial resolution, and of the HST public images, when available in the archive, for higher redshift galaxies. We excluded the sources for which a "compact" classification was given.

The resulting magnitudes show that NLS1s have typically lower luminosity bulges than S1s:

$$M_{B,bulge}(NLS1) = -18.54 \pm 1.06 \text{ vs. } M_{B,bulge}(S1) = -19.80 \pm 0.73.$$

Giving a realistic estimate of the magnitude errors is not an easy task. All our photometric data are taken from literature, based on CCD observations, and given mostly with accuracy  $< 0.05$  mag. But our  $M_B$  values are affected by additional errors, which are introduced by the application of the correction terms:  $\Delta m_A$ ,  $\Delta m_i$ ,  $\Delta m_G$ ,  $\Delta m_k$  and  $\Delta m_{bulge}$ .

Among them,  $\Delta m_i$  and  $\Delta m_k$  are both dependent on the morphological type  $T$ , and the error caused by a wrong classification will be typically lower than 0.1 mag.  $\Delta m_{bulge}$  is also a function of  $T$ , and increases strongly for late-type spirals. A maximum uncertainty  $\Delta T < 2$  in the morphological classification of our objects translates into errors  $< 0.5$  and  $< 1$  mag for early- and late-type spirals, respectively.  $\Delta m_A$  is dominated by the contribution of the AGN continuum, since the emission lines affect only  $\sim 10$  per cent of the total correction. Therefore  $\Delta m_A$  depends on the spectrophotometric calibration of the continuum, and e.g. an accuracy of 20 per cent will correspond to an uncertainty of  $\sim 0.2$  mag.

In Fig. 4 we plotted  $M_{B,bulge}$  values against  $\mathcal{M}_{BH}$ . NLS1s are represented by filled dots, while S1s by empty triangles. For completeness, we decided to include in this analysis a sample of 14 quasars (asterisks), whose  $\mathcal{M}_{BH}$  and  $M_B$  are given by Kaspi et al. (2000). The sources were selected from their list excluding those having a  $\mathcal{M}_{BH}$  error greater than the value itself. The absolute magnitudes were corrected for AGN contribution using only the measured continuum flux at  $5100\text{\AA}$ , available in the same paper (Table 4). As expected after having calculated the median values of the plotted physical quantities, NLS1s fall in the lower ranges of the plot, and are well separated by S1s both in BH mass and bulge luminosity values, even if a region of overlap inevitably exists. Moreover, NLS1s, S1s and quasars seem to be well correlated in the plane  $\mathcal{M}_{BH} - M_B$ . Therefore we attempted a least square fit (represented by the solid line in Fig. 4) considering all points together, and obtaining:

$$M_B = -2.32(\pm 0.18) \log(\mathcal{M}_{BH}) - 3.40(\pm 1.36) \quad (4)$$

with a correlation coefficient  $R = 0.91$ .

In order to check the consistence of this result, we first converted blue absolute magnitudes into V band, by applying the morphological type dependent B–V values given by Jahnke & Wisotzki



(2003, their Table 4), and we did a new fit:  $M_V = -2.48(\pm 0.19) \log(\mathcal{M}_{\text{BH}}) - 3.09(\pm 1.40)$ . Then we applied the standard relation:  $M_V = +4.83 - 2.5 \log(L_V/L_\odot)$  and a mass-to-luminosity conversion for bulges and spheroidal galaxies found by Magorrian et al. (1998):  $\log(\mathcal{M}/\mathcal{M}_\odot) = -1.11 + 1.18(\pm 0.03) \log(L/L_\odot)$ , obtaining as a result:

$$\log(\mathcal{M}_{\text{BH}}/\mathcal{M}_\odot) = 0.85(\pm 0.09) \log(\mathcal{M}_{\text{bulge}}/\mathcal{M}_\odot) - 2.25(\pm 0.88) \quad (5)$$

In Table 5 we compare our result with similar  $\mathcal{M}_{\text{BH}} \propto \mathcal{M}_{\text{bulge}}^\alpha$  relations investigated by other authors. We notice that Wandel (2002) and McLure & Dunlop (2002) obtained slopes of 0.74 and 0.88 respectively, which are consistent with our  $0.85 \pm 0.09$  value.

On the contrary Bian & Zhao (2003a) found a steeper relation ( $\alpha = 1.61 \pm 0.59$ ) for a sample of 22 Narrow Line AGNs. The lower number of points and the limited range of the bulge mass values in comparison with their scatter could be at the origin of this result. Indeed the slope of their relation shows an error significantly larger than those presented by other authors. A more stable and less uncertain fit can be obtained by considering also broad-line AGNs, therefore spanning a wider range in both the physical quantities, BH and bulge masses. Laor (2001) also found a steeper relation ( $1.36 \pm 0.15$ ). A possible explanation could be that the Kaspi et al. (2000) relation is defined by using monochromatic luminosity, while Laor (1998, 2001) started from bolometric luminosity and applied a constant to convert into  $L_\lambda(5100\text{\AA})$ .

### 3.2. Stellar velocity dispersion

Contrary to what happens for most of S1 galaxies (Nelson & Whittle 1995), measuring  $\sigma_*$  in NLS1s with optical spectra is very difficult and sometimes even impossible because of the presence of large and bright Fe II multiplets, which completely suppress the typically used stellar absorption lines, like *e.g.* [Mg I]  $\lambda 5175$  and Fe I  $\lambda 5269$  (Fig. 5). Moreover, NLS1s having bright Fe II show often the Ca II triplet ( $\lambda \sim 8550\text{\AA}$ ) in emission (Persson 1988), preventing the use of these lines which are generally seen in absorption in S1 galaxies.

As an alternative Nelson & Whittle (1996) have shown that the width of the narrow emission line [O III]  $\lambda 5007$  can replace  $\sigma_*$ , expressed in terms of  $\text{FWHM}([\text{O III}]\lambda 5007)/2.35$ , though the correlation between these two quantities is moderately strong with considerable scatter.

Assuming that [O III]  $\lambda 5007$  profiles are dominated by virial motion in the bulge potential, these authors investigated some possible secondary influences on NLR kinematics. For example, they noticed that Seyfert galaxies with high radio luminosity tend to have [O III]  $\lambda 5007$  widths broader than what expected in case of gravitational motion, because the gas kinematics can be influenced by the presence of a radio jet. They also stressed a slight tendency for barred and/or disturbed Seyfert galaxies to have broader [O III]  $\lambda 5007$  emission lines. Indeed Barnes & Hernquist (1991) pointed out that the distribution and kinematics of near-nuclear gas can be altered during galaxy interactions.

Since  $\sigma_*$  measurements are available in literature only for few Seyferts of our sample, we choose to use  $\text{FWHM}([\text{O III}]\lambda 5007)$  for the others. Then for each object we collected the values of their radio luminosity ( $L_{\text{radio}}$ ), taking them from FIRST survey catalog and NED, or , when no direct measurements were available, using a relationship between the radio luminosity at 1.49GHz and the  $L_{\text{FIR}}$  found by Malumyan & Panajyan (2000) for a sample of Seyfert galaxies:  $\log(L_{\text{radio}}) = 0.95(\pm 0.06)\log(L_{\text{FIR}}) - 12.84(\pm 2.07)$  . We calculated  $L_{\text{FIR}}$  using the fluxes at  $60\ \mu\text{m}$  and  $100\ \mu\text{m}$  extracted from the IRAS Point Source Catalogue and Faint Source Catalogue. The total flux  $S_{\text{FIR}}$  ( $40 - 120\ \mu\text{m}$ ) was computed by means of the relation (Helou, Soifer, & Rowan-Robinson 1985):  $S_{\text{FIR}} = 1.26 \times 10^{-14}(2.58S_{60} + S_{100})\ \text{W m}^{-2}$ , where  $S_{60}$  and  $S_{100}$  are the flux densities given in Jansky. The so obtained radio luminosities are listed in Tables 6 and 7. The logarithmic values of  $\sigma_*$  and  $\mathcal{M}_{\text{BH}}$  are plotted in Fig. 6, where we have excluded those objects with  $L_{\text{radio}} > 10^{22.5}\ \text{W Hz}^{-1}$ , as suggested by Nelson & Whittle (1996). NLS1 galaxies are represented by filled dots and S1s by empty triangles. In addition we included quasars from Kaspi et al. (2000) (asterisks) and nearby non active galaxies (empty stars) from Gebhardt et al. (2000a).

A least square fit of these values (Fig. 6, solid line) gave the following relation:

$$\log(\mathcal{M}_{\text{BH}}) = 3.70(\pm 0.37) \log(\sigma) - 0.68(\pm 0.80) \quad (6)$$

with a correlation coefficient  $R = 0.81$ .

This result is in agreement with Nelson (2000) and Wang & Lu (2001), who found  $\mathcal{M}_{\text{BH}} \propto \sigma_*^{3.70}$ , and with Gebhardt et al. (2000a), who found  $\mathcal{M}_{\text{BH}} \propto \sigma_*^{3.75}$  (Fig. 6, dotted line). The Merritt & Ferrarese (2001) and Tremaine et al. (2002) relations are also plotted in Fig. 6 for comparison (dashed line and dot-dashed line, respectively).

We notice a larger scatter in our relation with respect to Gebhardt et al. (2000a). This is mostly caused by the stellar velocity dispersions of NLS1 galaxies, whose values span a range similar to that of S1s. Contrary to what we obtained in § 3.1, this should suggest that NLS1 and S1 galaxies are separated when their BH masses are considered, but identical in their bulge properties. Moreover, all NLS1s remain below the fit with some of them closer to the line and, therefore, showing lower stellar velocity dispersions corresponding to lower BH masses, while other NLS1s have clearly larger  $\sigma_*$  than expected. This is likely the reason for having a zero point lower than the value obtained by Gebhardt et al. (2000a). A similar result was already obtained by Mathur et al. (2001), and very recently by Bian & Zhao (2003b), who used a large sample of low redshift NLS1s extracted from the Sloan Digital Sky Survey, and by Grupe & Mathur (2004), who used a sample of NLS1s extracted from the ROSAT All-Sky Survey. They found that NLS1s mostly deviate from the  $\mathcal{M}_{\text{BH}} - \sigma_*$  relation defined by Tremaine et al. (2002), showing  $\sigma_*$  values higher than expected.

A possible reason for this scatter could be a spectral resolution not sufficient to measure with high precision the low  $\sigma_*$  values predicted by the fit. This objection is well discussed and rejected by Grupe & Mathur (2004). Moreover, in our case, those targets observed at higher resolution

are just NLS1s, while S1s, even if observed at lower resolution, show a similar range of  $\sigma_*$  values. Another reason could be the fact that the  $\text{FWHM}([\text{O III}]) - \sigma_*$  correlation is not tight and never proved to be valid for NLS1s. Therefore, it is clear that to give a definitive answer, the stellar kinematics in NLS1s should be more carefully investigated by means of direct measurements of  $\sigma_*$ .

Combining (6) with  $\mathcal{M}_{\text{bulge}} \propto \sigma_*^{3.3}$  given by Wang, Biermann, & Wandel (2000, and references therein), who assumed virial equilibrium, and  $\mathcal{M} \propto L^{5/4}$  and  $R \propto L^{1/2}$  dependencies, we obtain  $\mathcal{M}_{\text{BH}} \propto \mathcal{M}_{\text{bulge}}^{1.12 \pm 0.11}$ , which is consistent with  $\mathcal{M}_{\text{BH}} \propto \mathcal{M}_{\text{bulge}}^{0.85 \pm 0.09}$  given in § 3.1. Moreover starting from equation (6) and converting the BH mass into luminosity by means of equation  $M_V - \log(\mathcal{M}_{\text{BH}})$  given in § 4.1, and the standard relation:  $M_V = +4.83 - 2.5 \log(L_V/L_\odot)$ , we obtain  $L \propto \sigma_*^{3.67}$ . This is perfectly in agreement with the Faber–Jackson relation,  $L \propto \sigma_*^n$ , where  $n \sim 3-4$ , which is important not only in terms of a distance indicator for elliptical galaxies, but also in studying the physical properties of bulges, as mentioned by Nelson & Whittle (1996).

#### 4. SUMMARY AND CONCLUSIONS

In this work we have investigated the nature of NLS1s by following an indirect way, that is by using the host galaxy properties to compare black hole masses in NLS1s, S1s and also quasars.

Starting from the assumption that the emission line clouds of BLR are gravitationally bound to the BH and in random motion, we have calculated BH masses of NLS1s obtaining a typical logarithmic value of  $6.65 \pm 0.64 M_\odot$ , which is almost one order of magnitude lower than the value obtained for S1s ( $7.37 \pm 0.62 M_\odot$ ). Simultaneously we have confirmed that NLS1s and S1s have quite similar nuclear luminosities: (in logarithm),  $43.51 \pm 0.65 L_\odot$  and  $43.08 \pm 0.45 L_\odot$  respectively.

The physical properties of the bulges were investigated in NLS1s and S1s by means of photometric and spectroscopic data.

Published total apparent B magnitudes were corrected for extinction, inclination, redshift and AGN contribution, and converted into absolute magnitudes. Then, the bulge magnitudes were calculated taking advantage of the empirical B/T – morphology relation given by Simien & de Vaucouleurs (1986), and used by several authors. We plotted these values against BH masses for NLS1s and S1s, adding quasars extracted from literature, and we found that NLS1s are mostly confined in the lower ranges of the  $\mathcal{M}_{\text{BH}} - M_B$  plane. This result suggests that NLS1s are characterized by less massive BHs hosted in less massive bulges than S1s. This is in agreement with previous findings of Wang & Lu (2001), who explored only the  $\mathcal{M}_{\text{BH}} - \sigma_*$  relation, and in contrast with Mathur et al. (2001) and Bian & Zhao (2003a), who claimed for NLS1s with lower  $\mathcal{M}_{\text{BH}}/\mathcal{M}_{\text{bulge}}$  ratios. It is not straightforward to justify the different results found by these authors. After a careful inspection of the effects introduced by each correction we applied to the photometric data of our targets, we can observe that the slightly different way we calculated the correction terms for AGN contribution and galaxy inclination seem to cause changes which roughly compensate each other. Therefore we guess that the main source of disagreement is the morphological classification, which strongly affects the

resulting bulge magnitudes by quantities in the range 0.25-0.5 dex for uncertainties discussed in § 3.1.

A fit of NLS1s, S1s and quasar values together shows a strongly correlated relation,  $M_B = -2.32(\pm 0.18) \log(\mathcal{M}_{\text{BH}}) - 3.40(\pm 1.36)$ , which leads to  $\mathcal{M}_{\text{BH}} \propto \mathcal{M}_{\text{bulge}}^{0.85 \pm 0.09}$ . Since the slope is close to unity, we do not confirm the results by Laor (2001) and Bian & Zhao (2003a) who found a significantly non-linear BH–bulge correlation.

The velocity dispersion of the bulge stellar component was also explored to check whether NLS1s have also  $\sigma_*$  values typically lower than those measured in S1s. Since few values of  $\sigma_*$  were available in literature, we had to calculate the others measuring the [O III] emission line widths, and assuming that the gas kinematics is dominated by the bulge potential. As done before, we plotted these values against BH masses, adding quasars and also nearby non-active galaxies, and obtaining a good correlation  $\mathcal{M}_{\text{BH}} \propto \sigma_*^{3.70 \pm 0.37}$ . Contrary to the previous result, NLS1s are not clearly separated from S1s in the  $\mathcal{M}_{\text{BH}} - \sigma_*$  plane. In particular they span similar ranges of  $\sigma_*$ , suggesting that their bulges are in this respect identical. Moreover, all NLS1s of our sample fall below the fit, showing  $\sigma_*$  values higher than expected, and also below the relations found by Gebhardt et al. (2000a), Merritt & Ferrarese (2001) and Tremaine et al. (2002), which on the contrary are well in agreement with our S1s values. This discrepancy between the two results could be caused by the assumption of [O III] widths as representative of the stellar kinematics. Indeed the [O III]- $\sigma_*$  conversion has a large scatter and is not yet proved to be valid for NLS1 galaxies. Therefore we stress the necessity to directly measure  $\sigma_*$ , for example observing NLS1s in spectral ranges different from the optical one.

Since both relations are based on important assumptions, which can introduce significant errors, at the moment it is not possible to favor one over the other. The fact that, according to our first result, NLS1 galaxies seem to have less massive bulges harboring equally less massive BHs than S1 galaxies, strongly indicates that the hypothesis of an inclination effect of a disk-like BLR on the narrowness of Balmer emission lines should be rejected, at least for most NLS1s. A pure selection effect is not expected to be related to the physical properties of the bulges, and therefore NLS1s should be just those S1s with intrinsically smaller bulges to justify the difference we observe between NLS1s and S1s. On the other hand, our second result confirms the smaller  $\mathcal{M}_{\text{BH}}/\mathcal{M}_{\text{bulge}}$  ratio in NLS1s, which led Mathur et al. (2001) and Grupe & Mathur (2004) to suggest an evolutionary scenario for these AGNs toward a S1 stage. In particular, NLS1s would be AGNs in a phase when BHs are growing independently from their hosting environment.

However, both cases support the general idea of NLS1s in terms of AGNs with less massive BHs accreting matter at high rates in order to maintain nuclear luminosities comparable to those of S1s, as we said above. Moreover, our results are not in conflict with the evolutionary scenario and sustain the idea that NLS1s are likely to be young S1s, even in case of a joined evolution of BH and bulge. In fact calculations by Bian & Zhao (2003a) suggest time scales of the order of some  $\sim 10^8$  yr for a NLS1 to become a S1. This time scale is in agreement with the growth time

of a spiral bulge through minor merger phenomena. Indeed Walker, Mihos, & Hernquist (1996) demonstrated through N-body simulations that a minor merger makes significant disturbances to the morphology of a larger galaxy in less than 1 Gyr of the onset of the merger. Moreover Aguerri, Balcells, & Peletier (2001) showed that the accretion of small satellites is an effective mechanism for the growth of bulges in spiral galaxies.

We are grateful to the referee for precious comments which improved the quality of the paper. VB is grateful to Y. Lu, S. Kaspi and T. Boller for valuable suggestions. SC is grateful to S. Temporin for having supported this work with useful discussions.

This research was partially based on data from the ING Archive.

In this work we have used the NASA/IPAC Extragalactic Database (NED) which is operated by the Jet Propulsion Laboratory, California Institute of Technology, under contract with the National Aeronautics and Space Administration.

This research has made use of the TARTARUS database, which is supported by Jane Turner and Kirpal Nandra under NASA grants NAG5-7385 and NAG5-7067.

## REFERENCES

- Aguerri, J. A. L., Balcells, M., & Peletier, R. F. 2001, *A&A*, 367, 428
- Barnes, J. E. & Hernquist, L. E. 1991, *ApJ*, 370, L65
- Bian, W. & Zhao, Y. 2003, *PASJ*, 55, 143
- Bian, W. & Zhao, Y. 2004, *MNRAS*, 347, 607
- Boller, T., Brandt, W. N., & Fink, H. 1996, *A&A*, 305, 53
- Boroson, T. A., & Green, R. F. 1992, *ApJS*, 80, 109
- Cardelli, J. A., Clayton, G. C., & Mathis, J. S. 1989, *ApJ*, 345, 245
- Crenshaw, D. M. et al. 2002, *ApJ*, 566, 187
- de Vaucouleurs, G., de Vaucouleurs, A., Corwin, H. G., Buta, R. J., Paturel, G., & Fouque, P. 1991, Volume 1-3, XII, 2069 pp. 7 figs.. Springer-Verlag Berlin Heidelberg New York
- Ferrarese, L. & Merritt, D. 2000, *ApJ*, 539, L9
- Gebhardt, K. et al. 2000a, *ApJ*, 539, L13
- Gebhardt, K. et al. 2000b, *ApJ*, 543, L5
- Granato, G. L., Zitelli, V., Bonoli, F., Danese, L., Bonoli, C., Delpino, F., 1993, *ApJS*, 89, 35

- Grupe, D. & Mathur, S. 2004, ApJ, submitted (astro-ph/0312390)
- Helou, G., Soifer, B. T., & Rowan-Robinson, M. 1985, ApJ, 298, L7
- Ho, L. 1999, ASSL Vol. 234: Observational Evidence for the Black Holes in the Universe, 157
- Kaspi, S., Smith, P. S., Netzer, H., Maoz, D., Jannuzi, B. T., & Giveon, U. 2000, ApJ, 533, 631
- Komossa, S. & Mathur, S. 2001, A&A, 374, 914
- Kormendy, J. & Richstone, D. 1995, ARA&A, 33, 581
- Jahnke, K. & Wisotzki, L. 2003, MNRAS, 346, 304
- Laor, A. 1998, ApJ, 505, L83
- Laor, A. 2001, ApJ, 553, 667
- Leighly, K. M. 1999, ApJS, 125, 317
- MacKenty, J. W. 1990, ApJS, 72, 231
- Magorrian, J. et al. 1998, AJ, 115, 2285
- Malumyan, V. H. & Panajyan, V. G. 2000, Astrophysics, 43, 403
- Mathur, S. 2000, MNRAS, 314, 17
- Mathur, S., Kuraszkiewicz, J., & Czerny, B. 2001, New Astronomy, 6, 321
- McLure, R. J., & Dunlop, J. S. 2001, MNRAS, 327, 199
- McLure, R. J. & Dunlop, J. S. 2002, MNRAS, 331, 795
- Merritt, D. & Ferrarese, L. 2001, ASP Conf. Ser. 249: The Central Kiloparsec of Starbursts and AGN: The La Palma Connection, 335
- Nelson, C. H. 2000, ApJ, 544, L91
- Nelson, C. H. & Whittle, M. 1995, ApJS, 99, 67
- Nelson, C. H. & Whittle, M. 1996, ApJ, 465, 96
- Osterbrock, D. E. 1989, Astrophysics of gaseous nebulae and active galactic nuclei, Mill Valley, CA, University Science Books
- Osterbrock, D. E., & Pogge, R. W. 1985, ApJ, 297, 166
- Padovani, P. & Rafanelli, P. 1988, A&A, 205, 53

- Persson, S. E. 1988, *ApJ*, 330, 751
- Peterson, B. M. 1993, *PASP*, 105, 247
- Peterson, B. M. & Wandel, A. 1999, *ApJ*, 521, L95
- Peterson, B. M. et al. 2000, *ApJ*, 542, 161
- Pounds, K. A., Stanger, V. J., Turner, T. J., King, A. R., & Czerny, B. 1987, *MNRAS*, 224, 443
- Prugniel, P. & Heraudeau, P. 1998, *A&AS*, 128, 299
- Schlegel, D. J., Finkbeiner, D. P., & Davis, M. 1998, *ApJ*, 500, 525
- Schmitt H. R. & Kinney, A. R. 2000, *ApJS*, 128, 479
- Simien, F. & de Vaucouleurs, G. 1986, *ApJ*, 302, 564
- Smith, J. E., Young, S., Robinson, A., Corbett, E. A., Giannuzzo, M. E., Axon, D. J., & Hough, J. H. 2002, *MNRAS*, 335, 773
- Strateva, I. V., Strauss, M. A., Hao, L., Schlegel, D. J. 2003, *AJ*, 126, 1720
- Tremaine, S. et al. 2002, *ApJ*, 574, 740
- Véron-Cetty, M.-P., Véron, P., & Gonçalves, A. C. 2001, *A&A*, 372, 730
- Vestergaard, M., Wilkes, B. J. & Barthel, P. D. 2000, *ApJ*, 538, 103
- Walker, I. R., Mihos, J. C., & Hernquist, L. 1996, *ApJ*, 460, 121
- Wandel, A. 1999, *ApJ*, 519, L39
- Wandel, A. 2002, *ApJ*, 565, 762
- Wandel, A., Peterson, B. M., & Malkan, M. A. 1999, *ApJ*, 526, 579
- Wang, Y. P., Biermann, P. L., & Wandel, A. 2000, *A&A*, 361, 550
- Wang, T. & Lu, Y. 2001, *A&A*, 377, 52
- Whittle, M. 1992, *ApJS*, 79, 49
- Winkler, H. 1997, *MNRAS*, 292, 273
- Wu, Xue-Bing & Han, J. L. 2001, *A&A*, 380, 31

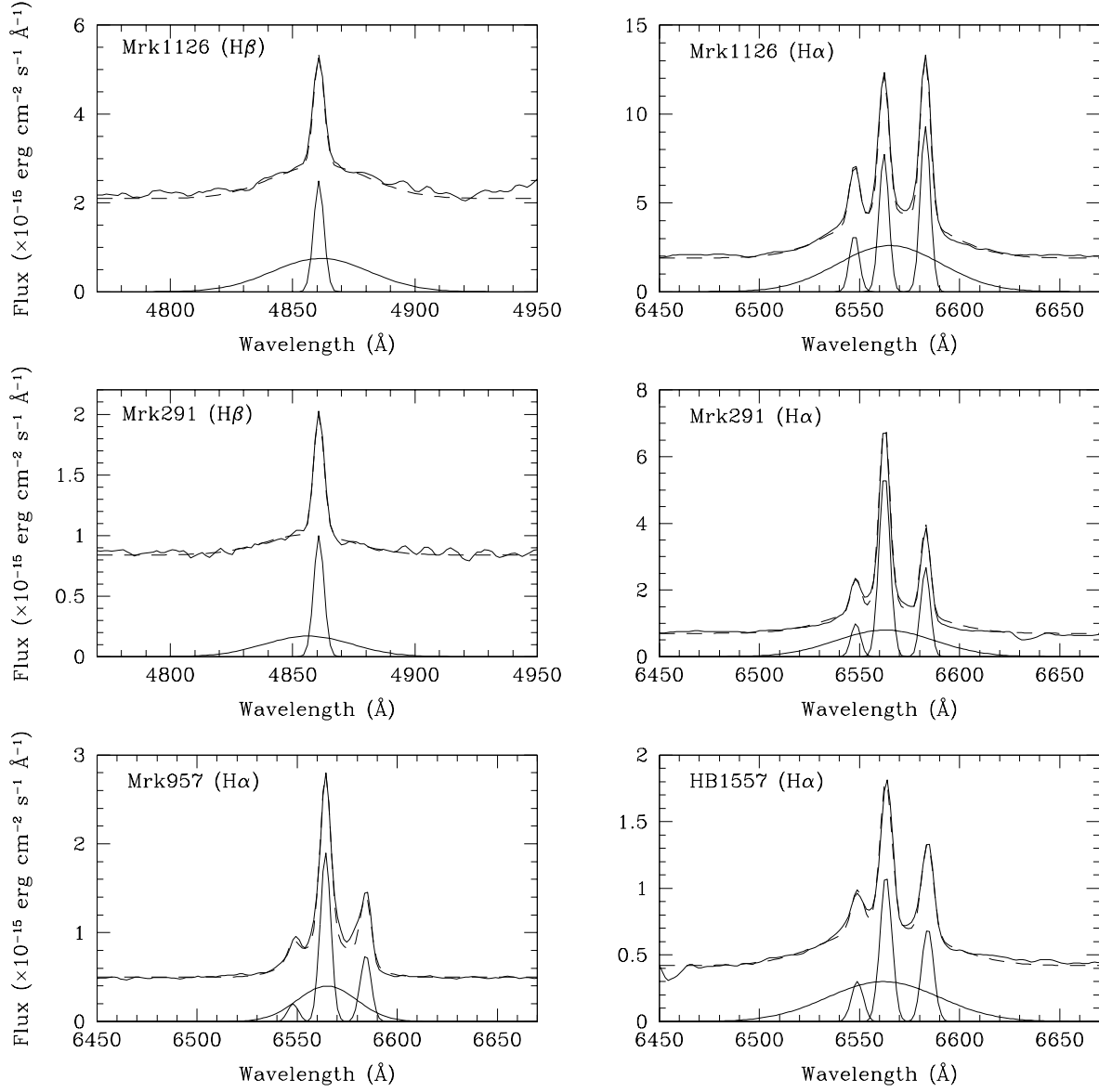


Fig. 1.— Multigaussian deblending of broad and narrow H $\beta$  and H $\alpha$  emission lines for the wrongly classified NLS1s. In each panel the observed profile (top) is compared with the fit (dashed line). Single gaussian components are also shown (bottom).



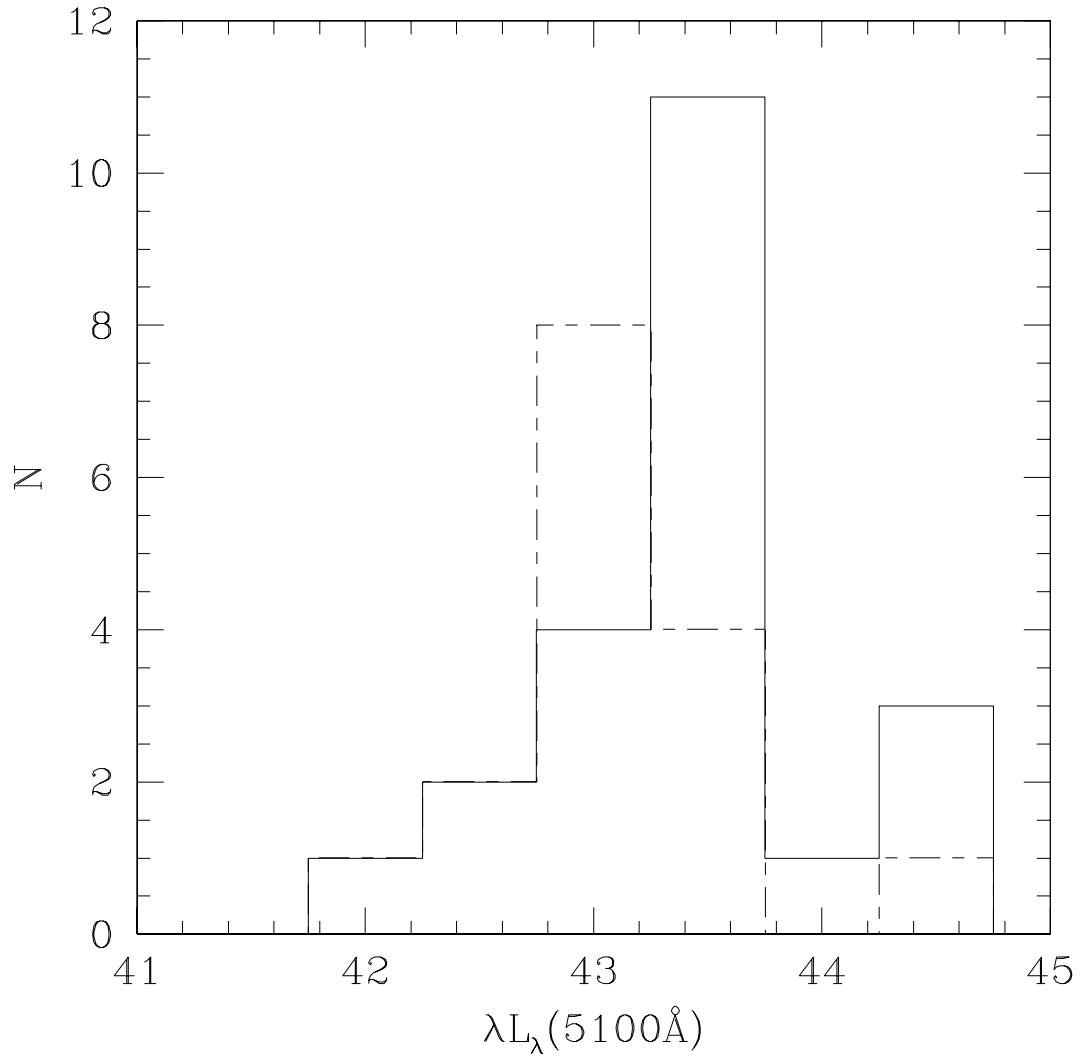


Fig. 2.— Comparison between the distributions of the measured nuclear continuum luminosity for NLS1 (solid) and S1 (dashed) galaxies. The median values are  $43.51 \pm 0.65$  and  $43.08 \pm 0.45$  respectively.

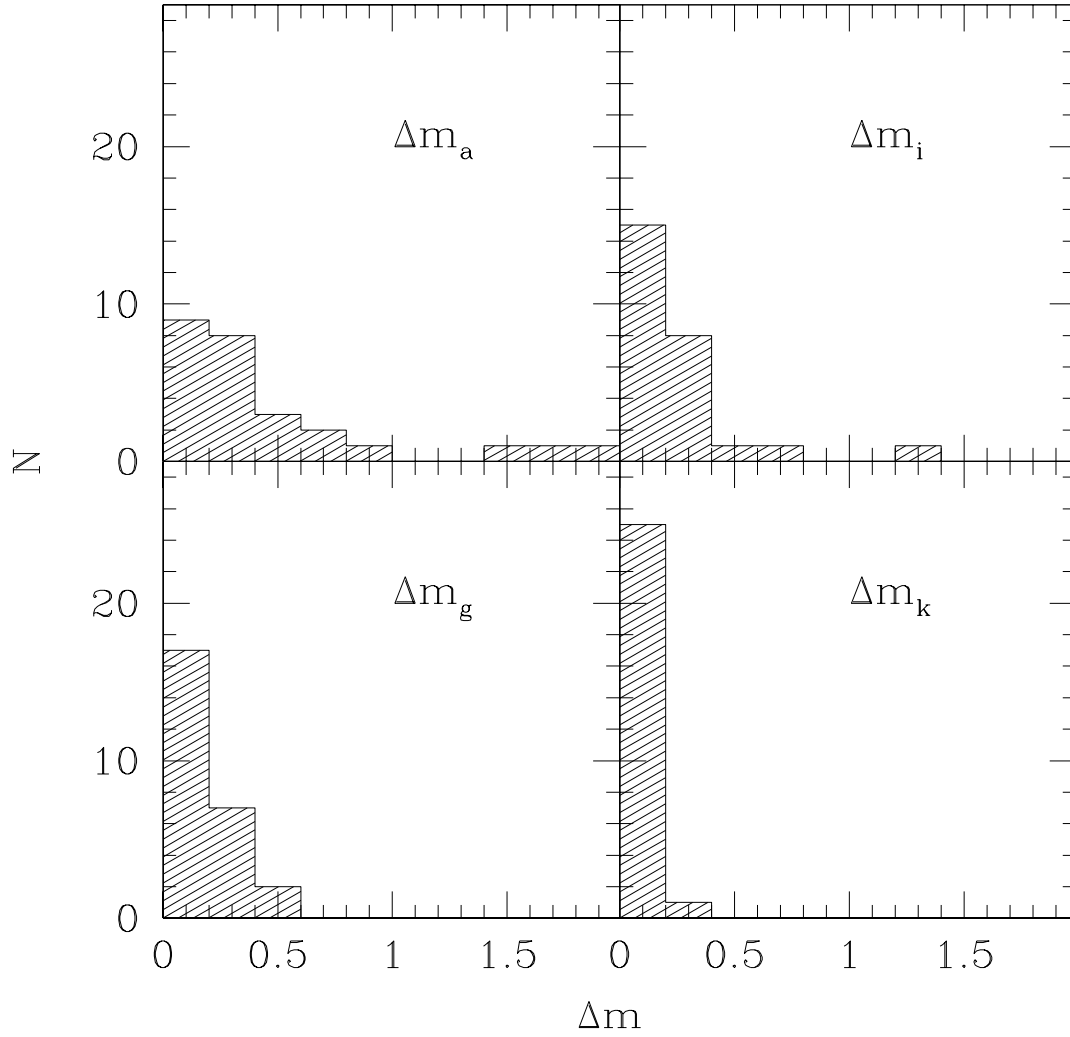


Fig. 3.— Distribution of magnitude correction terms applied to  $m_B$  values.

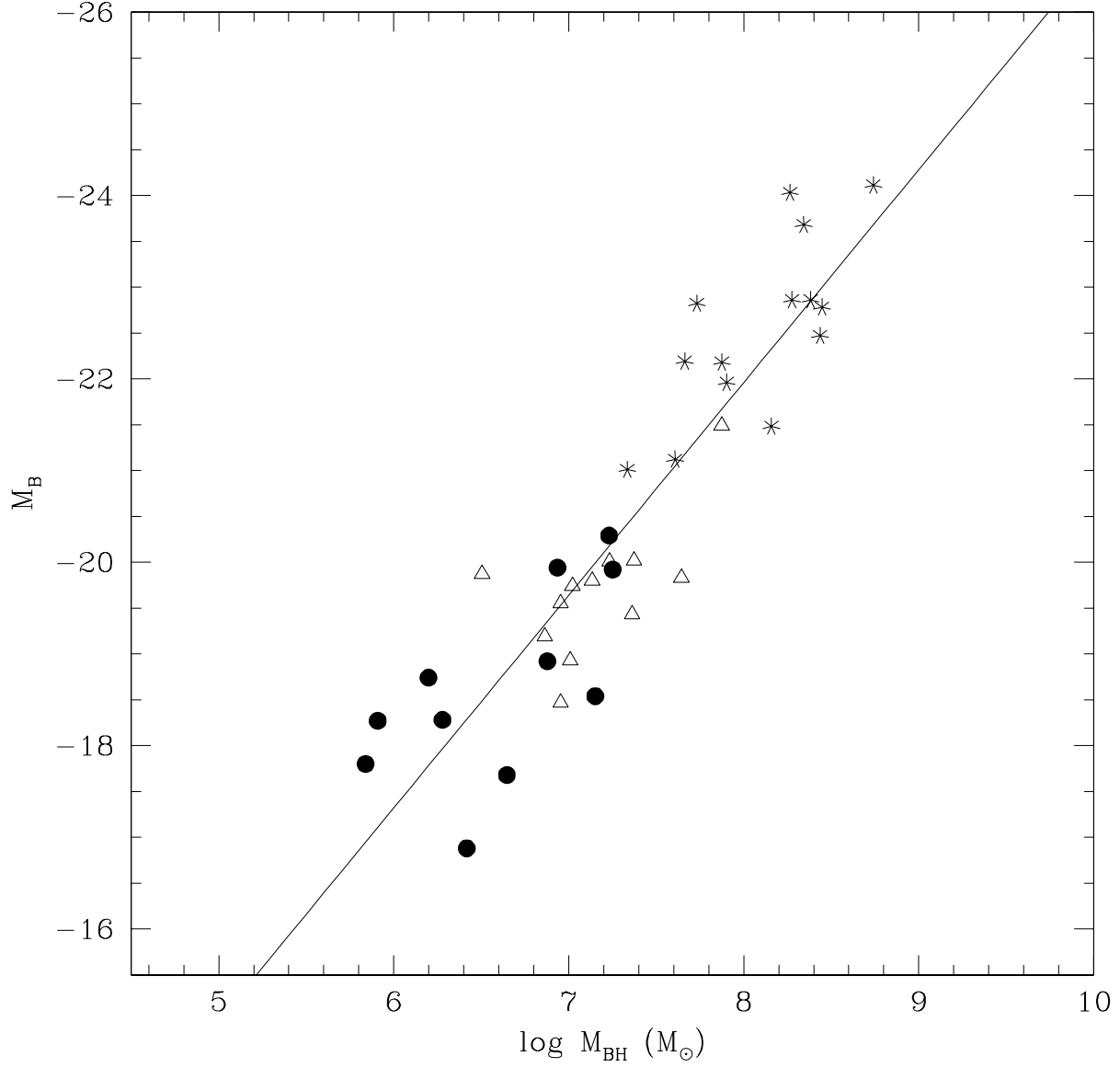


Fig. 4.—  $M_{\text{BH}} - M_{\text{B}}$  relation. NLS1s are indicated by filled circles, S1s by empty triangles and quasars by asterisks. The solid line represents a least square fit of the total sample of objects:  $M_{\text{B}} = -2.32(\pm 0.18) \log(M_{\text{BH}}) - 3.40(\pm 1.36)$ . The correlation coefficient is  $R = 0.91$ .

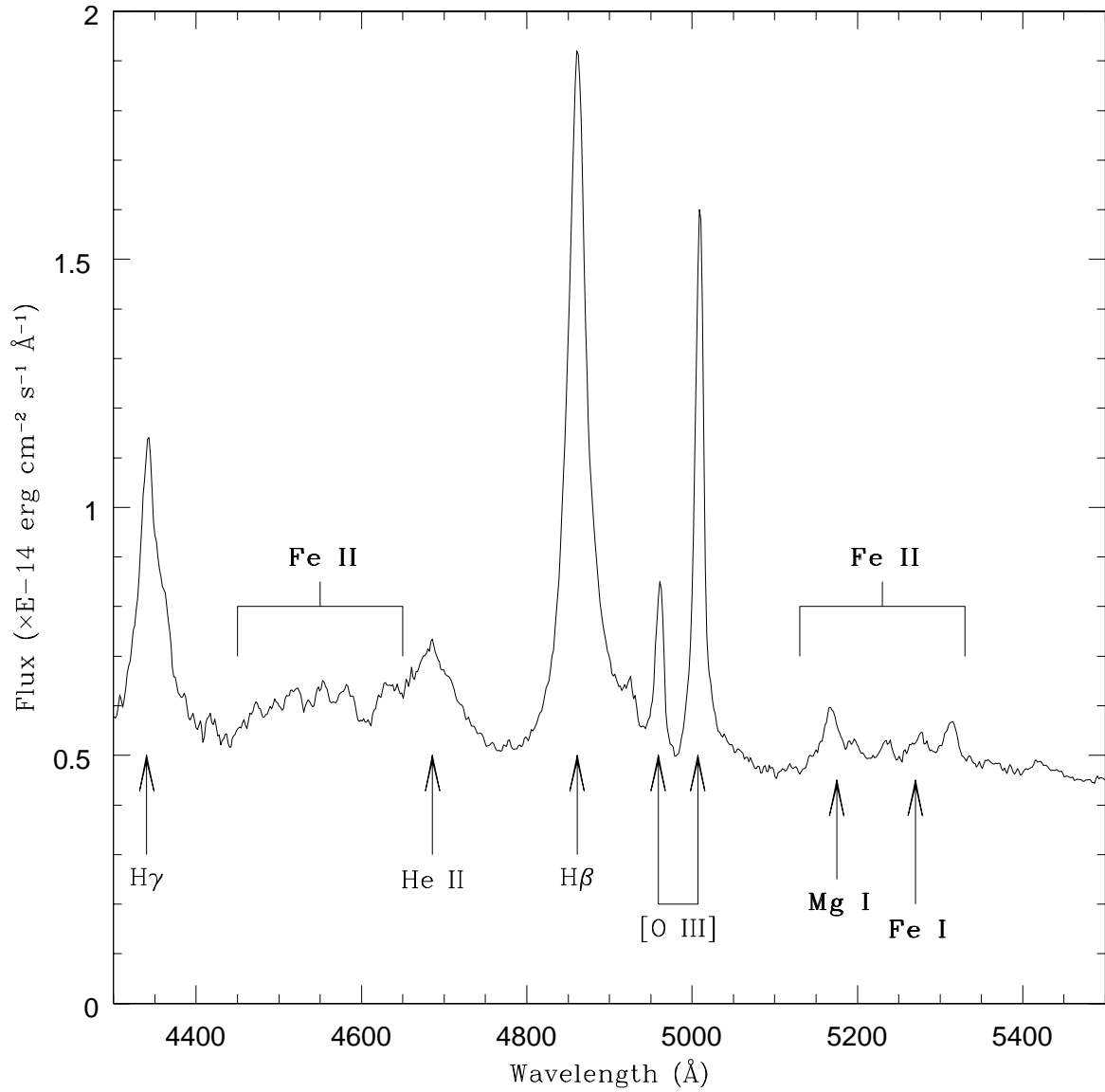


Fig. 5.— Nuclear spectrum of Mrk 335 showing strong Fe II multiplets. Arrows indicate emission lines, and the position of stellar absorption (Mg I and Fe I).

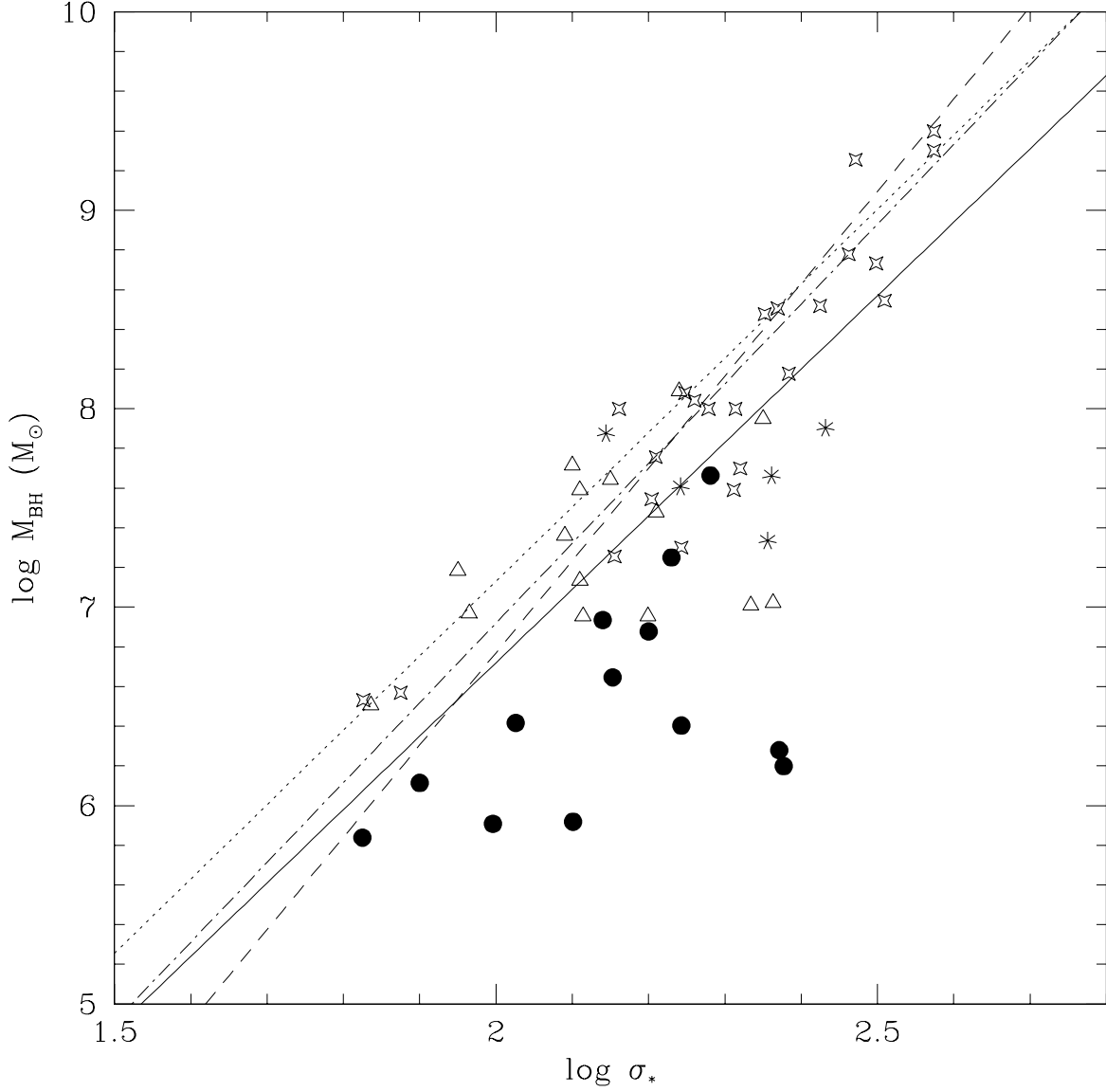


Fig. 6.—  $\mathcal{M}_{\text{BH}} - \sigma_*$  relation, where  $\sigma_*$  is intended in terms of  $\text{FWHM}([\text{O III}] \lambda 5007)$  in all objects for which it was not available in literature. Symbols are like in Fig.4, apart from empty stars which indicate nearby non active galaxies. The solid line is a least square fit of the total sample of objects:  $\log(\mathcal{M}_{\text{BH}}) = 3.70(\pm 0.37) \log(\sigma) - 0.68(\pm 0.80)$ . The correlation coefficient is  $R = 0.81$ . The relations found by Gebhardt et al. (2000a), Merritt & Ferrarese (2001) and Tremaine et al. (2002) are also plotted for comparison (dotted line, dashed line and dot-dashed line respectively).

Table 1. Narrow-Line Seyfert 1 – Observation Log.

Name	R.A.(J2000) (hh mm ss)	Dec.(J2000) (° ' ")	Telescope	Instrument	$\lambda$ range (Å)	Date	Exptime (sec)	$\Delta\lambda$ (Å)
Mrk335	00 06 19.5	+20 12 10	1.82m	AFOSC	4000-6500	2002 Sep 09	1800	12
					6000-8100	2002 Sep 09	1200	9
Mrk957	00 41 53.4	+40 21 18	INT	IDS	4400-6000	1996 Aug 08	1200	2.5
					6000-7600	1996 Aug 10	1200	2.5
IZW1	00 53 34.9	+12 41 36	INT	IDS	4400-6000	1996 Aug 08	1800	2.5
					5900-7500	1996 Aug 07	1200	2.5
Mrk359	01 27 32.5	+19 10 44	INT	IDS	4400-6000	1996 Aug 08	900	2.5
					5900-7500	1996 Aug 08	900	2.5
E0144	01 46 44.8	-00 40 43	INT	IDS	4400-6000	1996 Aug 09	1200	2.5
					5900-7500	1996 Aug 07	1200	2.5
Mrk1044	02 30 05.4	-08 59 53	INT	IDS	4400-6000	1996 Aug 08	900	2.5
					5900-7500	1996 Aug 06	900	2.5
IR04312	04 34 41.5	+40 14 22	1.82m	AFOSC	4000-6500	2002 Sep 10	1800	12
UGC3478	06 32 47.2	+63 40 25	1.82m	AFOSC	4000-6500	2003 Jan 27	1800	12
					6000-8100	2003 Jan 27	1200	9
Mrk705	09 26 03.3	+12 44 04	INT	IDS	4400-6000	1995 Jan 17	1500	3.5
Mrk142	10 25 31.3	+51 40 35	INT	IDS	4400-6000	1995 Jan 17	1800	4
					5850-7800	1995 Jan 17	1800	4
IC3599	12 37 41.2	+26 42 27	WHT	ISIS	3350-5900	1995 Mar 05	450	9
					5400-8350	1995 Mar 05	450	2.5
Mrk684	14 31 04.8	+28 17 14	INT	IDS	4200-7400	1996 Aug 11	1200	6.5
Mrk478	14 42 07.4	+35 26 23	INT	IDS	4100-7200	1996 Aug 10	900	6.5
Mrk291	15 55 07.9	+19 11 33	INT	IDS	4400-6000	1996 Aug 07	900	2.5
					5900-7500	1996 Aug 05	900	2.5
Mrk493	15 59 09.6	+35 01 48	INT	IDS	4400-6000	1996 Aug 06	900	2.5
					5900-7500	1996 Aug 08	900	2.5
Hb1557	15 59 22.2	+27 03 39	INT	IDS	4400-6000	1996 Aug 08	1200	2.5
					5900-7500	1996 Aug 08	1200	2.5
Kaz163	17 46 59.8	+68 36 39	INT	IDS	4400-5950	1996 Aug 07	1200	2.5
					5900-7450	1996 Aug 05	1200	2.5
Mrk507	17 48 38.4	+68 42 16	INT	IDS	4300-6000	1996 Aug 09	1200	2.5
					5900-7050	1996 Aug 07	900	2.5
Mrk896	20 46 20.9	-02 48 45	INT	IDS	4400-5950	1996 Aug 08	1200	2.5
					5900-7450	1996 Aug 06	1200	2.5
Ark564	22 42 39.3	+29 43 31	WHT	ISIS	4700-5550	1999 Jun 10	600	1.5
Ucm2257	22 59 32.9	+24 55 06	INT	IDS	4250-7450	1996 Aug 11	1800	2.5
Mrk1126	23 00 47.8	-12 55 07	INT	IDS	4400-6000	1996 Aug 09	1200	6.5
					5900-7500	1996 Aug 07	1200	2.5

Table 2. Seyfert 1 – Observation Log.

Name	R.A. (J2000) (hh mm ss)	Dec. (J2000) ( $^{\circ}$ ' ")	Telescope	Instrument	$\lambda$ range ( $\text{\AA}$ )	Date	Exptime (sec)	$\Delta\lambda$ ( $\text{\AA}$ )
Mrk1146	00 47 19.4	+14 42 13	1.82m	AFOSC	4000-6500	2002 Sep 30	1200	7.5
					6000-8100	2002 Sep 30	1200	5.5
UGC524	00 51 35.0	+29 24 05	1.82m	AFOSC	4000-6500	2003 Jan 26	1800	12
					6000-8100	2003 Jan 26	1200	9
Mrk975	01 13 51.0	+13 16 18	1.82m	AFOSC	4000-6500	2003 Jan 27	1800	12
					6000-8100	2003 Jan 27	1200	9
Mrk358	01 26 33.6	+31 36 59	1.82m	AFOSC	4000-6500	2002 Sep 30	1800	7.5
					6000-8100	2002 Sep 30	1200	5.5
Mrk1040	02 28 14.5	+31 18 42	1.82m	AFOSC	4000-6500	2002 Sep 30	1200	7.5
					6000-8100	2002 Sep 30	1200	5.5
UGC3142	04 43 46.8	+28 58 19	1.82m	AFOSC	6000-8100	2003 Jan 25	1800	12
					6000-8100	2003 Jan 25	1200	9
Mrk10	07 47 29.1	+60 56 01	INT	IDS	4400-5950	1995 Jan 14	1500	3.5
Mrk382	07 55 25.3	+39 11 10	1.82m	AFOSC	4000-6500	2003 Jan 25	1800	12
					6000-8100	2003 Jan 25	1200	9
Mrk124	09 48 42.6	+50 29 31	INT	IDS	4400-6000	1995 Jan 17	1500	3.5
NGC3080	09 59 55.8	+13 02 38	INT	IDS	4400-6000	1995 Jan 15	1800	3.5
Mrk40	11 25 36.2	+54 22 57	INT	IDS	4400-6000	1995 Jan 17	1500	3.5
Mrk205	12 21 44.0	+75 18 38	1.82m	AFOSC	4000-6500	2003 Jan 25	1800	12
					6000-8100	2003 Jan 25	1200	9
Ton730	13 43 56.7	+25 38 48	WHT	ISIS	3500-6000	1999 Mar 23	1200	4.0
					5800-8250	1999 Mar 23	1200	5.5
3C382	18 35 03.4	+32 41 47	WHT	ISIS	3700-5350	2000 Jul 06	600	2.5
					6000-7400	2000 Jul 06	600	4.5
3C390.3	18 42 09.0	+79 46 17	INT	IDS	4300-5800	1995 Jan 14	1800	3.5

Table 3. Photometric data of NLS1 and S1 galaxies.

Object	T	$m_B$	$\Delta m_A$	$\Delta m_i$	$\Delta m_g$	$\Delta m_k$	$m'_B$	$M_B$	$\Delta m_{bulge}$	$M_{B,bulge}$
Narrow-Line Seyfert 1										
Mrk335	0	14.20	0.36	0.00	-0.15	-0.12	14.29	-20.80	0.86	-19.94
IZw1	2	14.47	1.56	-0.17	-0.28	-0.18	15.41	-21.52	1.23	-20.29
Mrk359	3	14.52	0.67	-0.14	-0.23	-0.04	14.78	-19.34	1.54	-17.80
Mrk1044	1	14.64	0.39	-0.10	-0.15	-0.06	14.72	-19.30	1.02	-18.28
UGC3478	5	13.85	0.10	-0.64	-0.39	-0.05	12.87	-20.81	2.54	-18.27
Mrk142	1	16.06	0.69	-0.14	-0.07	-0.21	16.33	-19.94	1.02	-18.92
Mrk684	2	15.26	1.73	-0.20	-0.09	-0.14	16.56	-19.77	1.23	-18.54
Mrk493	4	14.79	0.37	-0.19	-0.11	-0.06	14.80	-20.71	1.97	-18.74
Mrk896	4	15.15	0.94	-0.37	-0.20	-0.05	15.47	-19.66	1.97	-17.68
Ark564	4	14.81	1.85	-0.26	-0.26	-0.04	16.10	-18.85	1.97	-16.88
Mrk590	1	14.45	0.04	-0.05	-0.16	-0.10	14.18	-20.94	1.02	-19.92
Seyfert 1										
Mrk1146	2	15.53	0.25	-0.23	-0.43	-0.12	15.00	-20.97	1.23	-19.74
UGC524	3	14.40	0.25	-0.05	-0.27	-0.09	14.24	-21.57	1.54	-20.02
Mrk975	1	15.67	0.26	-0.26	-0.11	-0.11	15.45	-21.02	1.02	-20.01
Mrk358	4	14.83	0.09	-0.19	-0.21	-0.09	14.43	-21.84	1.97	-19.87
Mrk1040	4	13.89	0.20	-1.32	-0.41	-0.03	12.33	-21.77	1.97	-19.80
Mrk10	4	14.53	0.18	-0.63	-0.20	-0.06	13.82	-21.52	1.97	-19.55
Mrk382	3	15.30	0.24	-0.06	-0.21	-0.06	15.18	-20.44	1.97	-18.47
Mrk124	3	15.94	0.53	-0.24	-0.06	-0.13	16.04	-20.73	1.54	-19.19
NGC3080	1	15.70	0.40	-0.03	-0.13	-0.13	15.82	-19.95	1.02	-18.93
Mrk205	1	15.23	0.20	-0.25	-0.18	-0.26	14.74	-22.51	1.02	-21.49
Mrk817	1	14.33	0.46	0.00	-0.03	-0.12	14.64	-20.85	1.02	-19.83
NGC3516	0	12.59	0.15	-0.08	-0.18	-0.04	12.44	-20.29	0.86	-19.43

Note. — Column: (1) – object name; (2) – morphological type; (3) – total apparent B magnitude; (4,5,6,7) – magnitude corrections for nuclear nonstellar continuum and emission lines ( $\Delta m_A$ ), inclination ( $\Delta m_i$ ), Galactic absorption ( $\Delta m_g$ ), and redshift ( $\Delta m_k$ ); (8) – total corrected apparent B magnitude; (9) – total corrected absolute B magnitude; (10) – correction to obtain bulge magnitude; (11) – bulge absolute B magnitude.



Table 4. Quasar sample.

Name	R.A. (hh mm ss)	Dec. (° ' ")	z	$f_\lambda(5100\text{\AA})$ ( $\text{erg cm}^{-2} \text{s}^{-1} \text{\AA}^{-1}$ )	$M_B$	$\log L_{1415}$ ( $\text{W Hz}^{-1}$ )	$\mathcal{M}_{BH}$ ( $10^7 M_\odot$ )	$\log \sigma_*$ ( $\text{km s}^{-1}$ )
PG0026...	00 29 13.6	+13 16 03	0.142	$2.7 \times 10^{-15}$	-22.82	23.71	$5.4^{+1.0}_{-1.1}$	...
PG0052...	00 54 52.1	+25 25 38	0.155	$2.1 \times 10^{-15}$	-23.68	22.95	$22.0^{+6.3}_{-5.3}$	...
PG0804...	08 10 58.6	+76 02 42	0.100	$5.5 \times 10^{-15}$	-22.86	22.64	$18.9^{+1.9}_{-1.7}$	...
PG0844...	08 47 42.4	+34 45 04	0.064	$3.7 \times 10^{-15}$	-21.01	21.79	$2.16^{+0.90}_{-0.83}$	2.356
PG0953...	09 56 52.4	+41 15 22	0.239	$1.6 \times 10^{-15}$	-24.03	23.77	$18.4^{+2.8}_{-3.4}$	...
PG1211...	12 14 17.7	+14 03 13	0.085	$5.7 \times 10^{-15}$	-21.12	22.47	$4.05^{+0.96}_{-1.21}$	2.242
PG1226...	12 29 06.7	+02 03 09	0.158	$21.3 \times 10^{-15}$	-24.11	27.67	$55.1^{+8.9}_{-7.9}$	...
PG1229...	12 32 03.6	+20 09 29	0.064	$2.1 \times 10^{-15}$	-22.18	22.12	$7.5^{+3.6}_{-3.5}$	2.144
PG1307...	13 09 47.0	+08 19 49	0.155	$1.8 \times 10^{-15}$	-22.78	22.63	$28^{+11}_{-18}$	...
PG1351...	13 53 15.8	+63 45 45	0.087	$5.1 \times 10^{-15}$	-22.19	22.29	$4.6^{+3.2}_{-1.9}$	2.361
PG1411...	14 13 48.3	+44 00 14	0.089	$3.7 \times 10^{-15}$	-21.96	22.38	$8.0^{+3.0}_{-2.9}$	2.432
PG1613...	16 13 57.2	+65 43 10	0.129	$3.5 \times 10^{-15}$	-22.86	23.41	$24.1^{+12.5}_{-8.9}$	...
PG1617...	16 20 11.3	+17 24 28	0.114	$1.4 \times 10^{-15}$	-22.47	22.85	$27.3^{+8.3}_{-9.7}$	...
PG2130...	21 32 27.8	+10 08 19	0.061	$4.8 \times 10^{-15}$	-21.48	22.56	$14.4^{+5.1}_{-1.7}$	...

Note. — Column: (1) – object name; (2,3) – right ascension and declination (J2000); (4) – redshift; (5) – continuum flux at  $\sim 5100\text{\AA}$ ; (6) – absolute B magnitude; (7) – logarithmic radio luminosity at 1415 MHz (Nelson 2000); (8) – estimated black hole mass in units of ( $10^7 M_\odot$ ); (9) – logarithmic stellar velocity dispersion obtained from FWHM([O III]) values by Nelson (2000).

Table 5.  $\mathcal{M}_{BH} \propto \mathcal{M}_{bulge}^\alpha$  for different authors.

Reference	Sample	N	$\alpha$	R
This work	NLS1s, S1s and quasars	37	$0.85 \pm 0.09$	0.91
Bian & Zhao (2003)	NL AGNs	22	$1.61 \pm 0.59$	0.74
Wandel (2002)	AGNs	47	$0.74 \pm 0.11$	0.67
McLure & Dunlop (2002)	AGNs	72	$0.88 \pm 0.06$	0.77
Laor (2001)	quasars & Seyfert	24	$1.36 \pm 0.21$	0.80
Laor (2001)	AGNs + Quiescent Galaxies	40	$1.54 \pm 0.15$	0.80

Note. — Column: (1) – bibliographic reference; (2) – sample; (3) – number of objects; (4) – exponent of  $\mathcal{M}_{BH} \propto \mathcal{M}_{bulge}^\alpha$  relation; (5) – correlation coefficient.

Table 6. Narrow-Line Seyfert 1 – Black hole masses and stellar velocity dispersions.

NLS1	$z$	$\lambda L_{\lambda}(5100\text{\AA})$ ( $\text{erg s}^{-1}$ )	$R_{BLR}$ (lt days)	$FWHM(H\beta)$ ( $\text{km s}^{-1}$ )	$M_{BH}$ ( $10^6 M_{\odot}$ )	$\log L_{radio}$ ( $\text{W Hz}^{-1}$ )	$\log \sigma_*$ ( $\text{km s}^{-1}$ )
Mrk335	0.0260	$3.1 \cdot 10^{43}$	$14.7 \pm 2.4$	2007.7	$8.61 \pm 0.84$	21.99 <sup>a</sup>	2.140
IZW1	0.0606	$29.2 \cdot 10^{43}$	$69.9 \pm 6.6$	1439.2	$17.00 \pm 5.06$	22.79 <sup>a</sup>	2.769
Mrk359	0.0167	$1.1 \cdot 10^{43}$	$7.1 \pm 0.9$	816.2	$0.69 \pm 0.09$	21.45 <sup>a</sup>	1.825
E0144	0.0827	$2.5 \cdot 10^{43}$	$12.6 \pm 1.3$	1566.2	$4.50 \pm 0.47$	22.75 <sup>b</sup>	2.132
Mrk1044	0.0159	$0.6 \cdot 10^{43}$	$4.6 \pm 0.7$	1684.6	$1.90 \pm 0.29$	21.09 <sup>b</sup>	2.371
IR04312	0.0201	$3.25 \cdot 10^{43}$	$15.0 \pm 1.4$	1373.7	$0.83 \pm 0.08$	22.14 <sup>a</sup>	2.101
UGC3478	0.0131	$0.3 \cdot 10^{43}$	$2.6 \pm 0.4$	1460.8	$0.81 \pm 0.10$	21.62 <sup>a</sup>	1.996
Mrk705	0.0287	$29.2 \cdot 10^{43}$	$68.3 \pm 6.3$	2153.5	$46.13 \pm 4.31$	22.13 <sup>b</sup>	2.281
Mrk142	0.0448	$3.3 \cdot 10^{43}$	$15.2 \pm 1.4$	1876.3	$7.54 \pm 0.72$	21.36 <sup>b</sup>	2.200
IC3599	0.0224	$0.1 \cdot 10^{43}$	$1.7 \pm 0.3$	692.9	$0.13 \pm 0.02$	...	2.055
Mrk684	0.0463	$8.7 \cdot 10^{43}$	$9.8 \pm 1.9$	1805.6	$14.17 \pm 0.91$	22.52 <sup>c</sup>	2.669
Mrk478	0.0774	$28.9 \cdot 10^{43}$	$69.4 \pm 6.5$	1979.2	$30.60 \pm 3.34$	22.58 <sup>b</sup>	2.786
Mrk493	0.0316	$2.1 \cdot 10^{43}$	$11.1 \pm 1.2$	989.9	$1.58 \pm 0.02$	21.81 <sup>b</sup>	2.377
Kaz163	0.0637	$3.3 \cdot 10^{43}$	$15.3 \pm 1.5$	1844.8	$8.76 \pm 0.83$	22.80 <sup>c</sup>	2.332
Mrk507	0.0553	$3.2 \cdot 10^{43}$	$15.0 \pm 1.4$	1876.3	$9.44 \pm 1.04$	22.52 <sup>c</sup>	2.519
Mrk896	0.0265	$2.0 \cdot 10^{43}$	$10.6 \pm 1.1$	1673.4	$4.43 \pm 0.48$	21.47 <sup>c</sup>	2.153
Ark564	0.0244	$4.2 \cdot 10^{43}$	$17.9 \pm 1.6$	971.6	$2.61 \pm 0.26$	22.00 <sup>c</sup>	2.026
Ucm2257	0.0336	$1.6 \cdot 10^{43}$	$9.2 \pm 1.1$	1375.3	$2.53 \pm 0.30$	22.47 <sup>c</sup>	2.243
NGC4051	0.0023	...	...	...	$1.30 \pm 0.10^d$	20.29 <sup>b</sup>	1.90 <sup>e</sup>
Mrk590	0.0264	...	...	...	$17.8 \pm 0.38^d$	22.12 <sup>b</sup>	2.23 <sup>e</sup>

Note. — Column: (1) – object name; (2) – redshift; (3) – continuum luminosity at 5100Å; (4) – the estimated size of broad line region in light-days; (5) –  $H\beta$  line width in  $\text{km s}^{-1}$ ; (6) – the estimated black hole mass; (7) – the logarithmic value of stellar velocity dispersion measured from  $FWHM([\text{O III}]\lambda 5007)$ .

<sup>a</sup> $L_{radio}$  taken from NED

<sup>b</sup> $L_{radio}$  taken from FIRST catalog

<sup>c</sup> $L_{radio}$  derived from  $L_{FIR}$

<sup>d</sup>Black hole masses taken from Wu & Han (2001)

<sup>e</sup>Stellar velocity dispersions taken from Wandel (2002)

Table 7. Seyfert 1 – Black hole masses and stellar velocity dispersions.

S1	z	$\lambda L_{\lambda}(5100\text{\AA})$ ( $\text{erg s}^{-1}$ )	$R_{BLR}$ (lt days)	$FWHM(H\beta)$ ( $\text{km s}^{-1}$ )	$M_{BH}$ ( $10^7 M_{\odot}$ )	$\log L_{radio}$ ( $\text{W Hz}^{-1}$ )	$\log \sigma_*$ ( $\text{km s}^{-1}$ )
Mrk1146	0.0391	$1.1 \cdot 10^{43}$	$7.2 \pm 0.9$	3141.6	$1.05 \pm 1.35$	21.70 <sup>a</sup>	2.363
UGC524	0.0366	$1.6 \cdot 10^{43}$	$9.3 \pm 1.1$	4160.6	$2.36 \pm 0.34$	22.62 <sup>a</sup>	2.350
Mrk975	0.0492	$1.4 \cdot 10^{43}$	$8.3 \pm 1.0$	3775.4	$1.71 \pm 0.24$	22.75 <sup>a</sup>	2.577
Mrk358	0.0452	$0.7 \cdot 10^{43}$	$5.2 \pm 0.7$	2234.8	$0.32 \pm 0.05$	22.32 <sup>c</sup>	1.836
Mrk1040	0.0164	$0.8 \cdot 10^{43}$	$5.7 \pm 0.8$	4220.1	$1.36 \pm 0.20$	21.90 <sup>a</sup>	2.110
UGC3142	0.0218	$1.0 \cdot 10^{43}$	$6.6 \pm 1.7$	10488.5	$8.91 \pm 0.22$	22.36 <sup>a</sup>	2.350
Mrk10	0.0293	$1.2 \cdot 10^{43}$	$7.5 \pm 0.9$	3046.9	$0.90 \pm 0.12$	22.27 <sup>c</sup>	2.114
Mrk382	0.0332	$1.2 \cdot 10^{43}$	$7.4 \pm 0.9$	2903.3	$0.90 \pm 0.07$	21.86 <sup>c</sup>	2.199
Mrk124	0.0564	$3.0 \cdot 10^{43}$	$14.1 \pm 1.3$	1982.3	$0.73 \pm 0.02$	22.55 <sup>b</sup>	2.411
NGC3080	0.0355	$1.1 \cdot 10^{43}$	$6.9 \pm 0.9$	3172.4	$1.02 \pm 1.03$	22.06 <sup>c</sup>	2.334
Mrk40	0.0206	$0.3 \cdot 10^{43}$	$3.5 \pm 0.8$	4042.3	$0.93 \pm 0.13$	21.10 <sup>b</sup>	1.965
Mrk205	0.0703	$4.9 \cdot 10^{43}$	$19.9 \pm 1.7$	5082.9	$7.48 \pm 0.31$	22.67 <sup>c</sup>	2.275
Ton730	0.0853	$2.4 \cdot 10^{43}$	$11.8 \pm 1.6$	3761.6	$2.43 \pm 0.17$	22.78 <sup>c</sup>	2.233
3C390.3	0.0559	$5.5 \cdot 10^{43}$	$21.8 \pm 1.6$	5284.7	$22.3 \pm 2.4$	25.82 <sup>a</sup>	2.336
3C382	0.0559	$23.6 \cdot 10^{43}$	$60.3 \pm 5.3$	15991.4	$224.60 \pm 16.31$	25.49 <sup>a</sup>	2.616
Mrk79	0.0222	...	...	...	$5.20 \pm 2.40^d$	22.15 <sup>b</sup>	2.10 <sup>e</sup>
3C120	0.0330	...	...	...	$3.00 \pm 1.30^d$	...	2.21 <sup>e</sup>
Mrk817	0.0314	...	...	...	$4.40 \pm 1.20^d$	22.24 <sup>b</sup>	2.15 <sup>e</sup>
NGC3227	0.0038	...	...	...	$3.90 \pm 3.00^d$	21.36 <sup>b</sup>	2.11 <sup>e</sup>
NGC3516	0.0088	...	...	...	$2.30 \pm 0.90^d$	...	2.09 <sup>e</sup>
NGC5548	0.0171	...	...	...	$12.30 \pm 1.60^d$	22.14 <sup>b</sup>	2.24 <sup>e</sup>
NGC4151	0.0033	...	...	...	$1.53 \pm 0.93^d$	21.84 <sup>b</sup>	1.95 <sup>e</sup>

Note. — As in Table 6